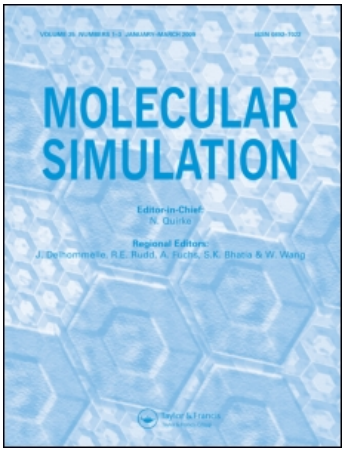

Molecular Simulation
Publication details, including instructions for authors and subscription information:
http://www.informaworld.com/smpp/title~content=t713644482

A DMol³ study of the methanol addition-elimination oxidation mechanism by methanol dehydrogenase enzyme

N. B. Idupulapati[a]; D. S. Mainardi[b]
[a] Institute for Micromanufacturing, Louisiana Tech University, Ruston, USA [b] Chemical Engineering Program, Institute for Micromanufacturing, Louisiana Tech University, Ruston, USA

To cite this Article Idupulapati, N. B. and Mainardi, D. S.(2008) 'A DMol³ study of the methanol addition-elimination oxidation mechanism by methanol dehydrogenase enzyme', Molecular Simulation, 34: 10, 1057 — 1064
To link to this Article: DOI: 10.1080/08927020802235656
URL: http://dx.doi.org/10.1080/08927020802235656

Molecular Simulation
Vol. 34, Nos. 10–15, September–December 2008, 1057–1064

Taylor & Francis
Taylor & Francis Group

A DMol^3 study of the methanol addition–elimination oxidation mechanism by methanol dehydrogenase enzyme

N.B. Idupulapati[a] and D.S. Mainardi[b]*

[a]*Institute for Micromanufacturing, Louisiana Tech University, Ruston, USA;* [b]*Chemical Engineering Program, Institute for Micromanufacturing, Louisiana Tech University, Ruston, USA*

(*Received 30 January 2008; final version received 27 May 2008*)

The addition–elimination (A–E) mechanism proposed for the oxidation of methanol to formaldehyde by PQQ-containing methanol dehydrogenase (MDH) enzyme is investigated at the Becke–Lee–Yang–Parr/double numerical with polarisation density functional theory level with the DMol^3 module of the Materials Studio® software. Two different models representing the *Methylobacterium extorquens* MDH (1H4I) active site are considered and tested upon methanol oxidation in gas phase. Model A consists of the PQQ molecule, the Ca^{2+} ion and aspartic acid (ASP-303), and model B contains also glutamic acid (GLU-177) and asparagine (ASN-261) in addition to the contents of model A. The first proton transfer from methanol to ASP-303 and from ASP-303 to PQQ is affected by the model size; however, the second proton transfer corresponding to the cleavage of C_{met}—H17 is practically unaffected by the MDH active site model under consideration. The energy barrier for the cleavage of the C atom of methanol (C_{met}) and H17 is 13 and 17 kcal/mol for models A and B, respectively, in good agreement with the general kinetic requirements of an enzymatic process. Step 1 as proposed in the literature is not kinetically favourable in the gas phase at this theory level. It is possible then, that either solvent effects are critical or that one or more intermediate steps leading to the formation of the first intermediate complex are missing from the proposed methanol A–E mechanism for the oxidation of methanol by MDH.

Keywords: oxidation mechanism; MDH; methanol; DFT; BLYP

1. Introduction

Methanol dehydrogenase (MDH) is a water soluble quinoprotein able to oxidise methanol, and other primary alcohols to their corresponding aldehydes [1]. The crystal structure of MDH from *Methlylobacterium extorquens* [2–4] and from *Methylophilus W3A1* [5,6] has been characterised using X-ray crystallographic methods. MDH has an $\alpha_2\beta_2$ tetrameric structure; each α subunit (66 kDa) contains one molecule of pyrroloquinoline quinone (PQQ) as its co-factor and one Ca^{2+} ion (Figure 1(a),(b)). The β-subunit is very small (8.5 kDa) and folds around the α -subunit; it cannot be reversibly dissociated, its function is unknown and it is not present in any other quinoproteins [2–4,7]. The Ca^{2+} ion in the MDH active site is electrostatically bonded to the C5 quinone oxygen (O5), the oxygen of the C10 carboxylate (O10), the nitrogen (N6) of the PQQ, the oxygen atoms (O12 and O13) from the carboxylate of Glu-177, and the oxygen (O11) of Asn-261 (Figure 1(b)) [2]. Apart from holding the PQQ molecule in place in the active site, the Ca^{2+} is believed to have an important role in the electro-oxidation reaction mechanism [7].

Two possible mechanisms for methanol oxidation by MDH have been proposed in the literature, the addition–elimination (A–E) and the hydride transfer (H-T) mechanisms [1,7]. The A–E is a three-step mechanism (Figure 2) that involves a proton transfer from methanol to an active site base, which is proposed to be Asp-303. It is believed that the presence of this catalytic base at the MDH active site initiates the oxidation reactions by subtracting a proton (H16) from methanol. This proton 'addition' to Asp-303 leads to the formation of a covalent hemiketal intermediate, since the resulting oxyanion ($O16^-$) in the methanol molecule is then attracted to the C5 of PQQ (Figure 2). The second step consists of the proton (H16) 'elimination' from Asp-303 and transfer to O5 of PQQ, and the final step is characterised by a second proton (H17) transfer from the methanol molecule to the O4 of PQQ, resulting in the formation of the by-product formaldehyde (CH_2O) [1,7]. The H-T is proposed to be a four-step mechanism (not shown). The first step involves two proton transfers: H16 and H17 from the methanol molecule to ASP-303 and C5 of PQQ, respectively, resulting in the formation of the by-product formaldehyde [1,7]. In the second step, there is a proton (H16) transfer from ASP-303 to the C5 of PQQ. The third step involves the proton (H17) transfer from the C5 of PQQ to ASP-303, and the final step consists of the transfer of H17 from ASP-303 to the O4 of PQQ. Irrespective of the mechanism under consideration, the rate-determining step for methanol oxidation by MDH is believed to be the

*Corresponding author. Email: mainardi@latech.edu

ISSN 0892-7022 print/ISSN 1029-0435 online

DOI: 10.1080/08927020802235656
http://www.informaworld.com

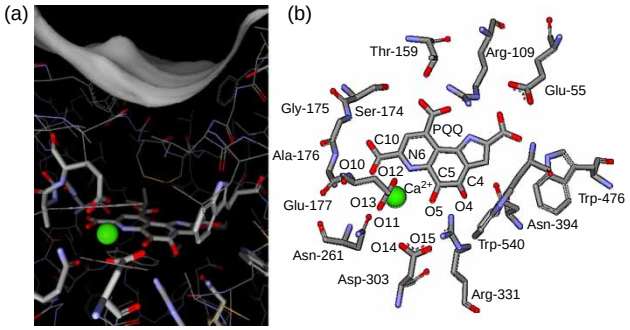

Figure 1. (a) View of the inside of the enzyme with the active site in stick model. The solid surface represents the external surface of the MDH enzyme from *M. extorquens* [2] showing the binding pocket. (b) View of the entire MDH active site from the binding pocket. Amino acids labels denote their location in the sequence obtained from the entry 1H4I of the protein data bank [2].

breaking of the C_{met}—H17 bond leading to the second proton transfer, which occurs in step 3 (Figure 2) and 1 of the A–E and H-T mechanisms, respectively [7].

Even though the H-T-type seems to be the mechanism that operates for the oxidation of glucose by glucose dehydrogenase [8,9] and other closely related type II alcohol dehydrogenases [10], the A–E methanol oxidation mechanism appears to be the preferred one by MDH. Experimental studies by Frank et al. [11] on methanol oxidation mechanisms by MDH found that the C5 carbonyl of the isolated PQQ molecule is very reactive towards nucleophilic reagents, suggesting that a covalent PQQ-substrate complex (hemiketal intermediate) formation would be possible in agreement to the A–E mechanism [11]. This hemiketal complex formation was also anticipated since the absorption and fluorescence spectra of covalent adduct of PQQ and methanol are almost identical to MDH-methanol complexes spectra, in favour of the A–E over the H-T mechanism [12,13]. Itoh et al. [14,15] from their theoretical and spectroscopic measurements showed that PQQ systems in organic solution can oxidise methanol, ethanol and 2-propanol to their corresponding aldehydes via the A–E mechanism. These authors reported that the crystal structure of one of the isolated hemiketal adducts showed methanol bound to C5 of PQQ. Crystallographic studies by Xia et al. [6] on MDH from *Methylophilus W3A1* in the presence of methanol indicated that in the MDH–PQQ–methanol complex, the methanol hydroxyl group is closer to the PQQ C5 atom (3.1 Å) than the methyl group (3.9 Å). According to these authors, the hydride ion transfer (H17 to C5 of PQQ) from the more distant methyl group of methanol would not be possible, supporting the formation of a hemiketal intermediate as suggested by the A–E mechanism.

Goodwin et al. [16] performed experimental kinetics and thermodynamic calculations on the whole Ca^{2+}-MDH enzyme in the presence of ammonium chloride solution and methanol. The reported activation energy for the oxidation of methanol at pH 9 was 35.4 kJ/mol,[16] however these authors did not particularly relate this activation energy to a step of the methanol oxidation mechanisms already proposed in the literature [16]. Recently Leopoldini et al. [17] theoretically investigated the two proposed A–E and H-T mechanisms at the B3LYP density functional theory (DFT) level and 6-31 + G* basis set for all atoms except calcium (LANL2DZ was used). Their model for the MDH active site included the PQQ cofactor, the Ca^{2+} ion, the residues having coordination with the calcium ion (GLU-171, ASN-261 and ASP-303) and also five nearby residues which form a sphere around the PQQ molecule (ARG-331, GLU-55, ARG-109, THR-153 and SER-174). In their calculations, however, only the reactive groups (CH_3COO^- and NH_3COCH_3) of the residues having coordination with the calcium ion and the PQQ molecule were considered in the calculation, and one hydrogen atom of each reactive group were frozen to prevent unreliable expansion of model during optimisation procedure [17]. Their calculated energy barriers for the rate-determining step, i.e. for the cleavage of C_{met}—H17 bond of methanol for the two proposed mechanisms (34.6 kcal/mol for A–E, 32.3 kcal/mol for H-T) were well above the general kinetic requirements of an enzymatic catalytic process (15–20 kcal/mol). So, they postulated an alternative mechanism, A–E-protonation, in which the

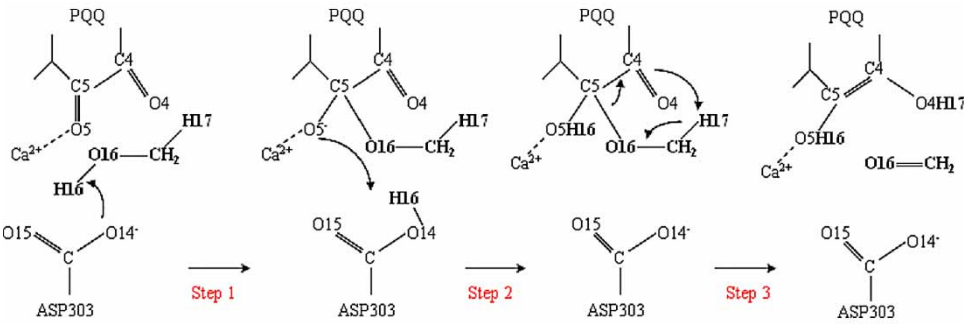

Figure 2. A–E oxidation mechanism proposed for MDH [1].

first step is the same as in the A–E mechanism (step 1), but the second step consists of the proton (H17) 'elimination' from the hemiketal methyl group and transfer to O4. The final step is characterised by the proton transfer (H16, 'protonation') from the ASP-303 to the O5 of PQQ. This new proposed mechanism reduced the energy barrier of the rate-determining step to 16 kcal/mol [17].

To the best of our knowledge, no clear theoretical evidence connecting the experimental observation in favour of the A–E methanol oxidation mechanism by MDH has been reported in the literature, being this the motivation of this paper. In this theoretical work, two MDH active site models are considered based on the exposed residues methanol molecules face upon approaching the active site through the enzyme binding pocket (Figure 1(a),(b)). No constrains (frozen atoms) are imposed during the geometry optimisation calculations using DFT. The A–E mechanism is tested for both MDH models in the presence of methanol and energy barriers are calculated and reported for each step in the mechanism.

2. Methodology

The Generalized Gradient Approximation [18] within the DFT formalism [19] is implemented in this study as provided by the module DMol^3 in Materials Studio® software developed by Accelrys, Inc. [20]. All geometry optimisation calculations are performed using the Becke–Lee–Yang–Parr (BLYP) exchange correlation functional [21] and the double numerical with polarisation (DNP) basis set since it is the best set available in DMol^3. This basis set considers a polarisation *d* function on heavy atoms and a polarisation *p* function on hydrogen atoms. It compares to the split-valence double zeta 6-31G** in size; however it is more accurate than the Gaussian basis sets of the same size [22]. When the BLYP/DNP theory level is used, errors are expected to be in the second decimal for calculated bond lengths (Å) and in the order of 4–10 (kcal/mol) in absolute energies, similar to those expected when using Becke-3 hybrid functionals and the 6-31G** basis set [23]. Harmonic vibrational frequency calculations are performed to ensure that stationary points on the potential energy surface of the systems are in fact local minima (all real frequencies) or transition states (only one imaginary frequency). Spin multiplicity states are also checked in all calculations and ground state geometries are presented.

Appropriate reactants and products involved in each step of the A–E mechanism are considered for defining atom pairing, so that a 3D trajectory file representing the reaction path preview is generated for each step with the Reaction Preview tool of the Materials Studio software. Then, these 3D trajectory files are used as inputs to obtain the corresponding transition states, using the linear synchronous transit and quadratic synchronous transit (LST/QST) calculation with conjugate gradient minimisation [24] within the Transition State search tool in DMol^3. This methodology starts with a LST/optimisation (bracketing the maximum between the reactant and product and performing energy minimisation of the obtained maximum in the reaction pathway). The Transition State hence obtained is used as starting point for performing a finer search with the QST/optimisation followed by a conjugate gradient minimisation. This cycle is repeated until a stationary point with only one imaginary frequency (transition state) is found [24], since in many cases several imaginary frequencies are found. In the later situation, the corresponding (imaginary) modes of vibrations are animated in order to visualise the mode that would eventually follow the intended step from a particular reactant to product. That particular mode is then selected to perform the transition state optimisation to verify whether the obtained geometry is indeed a transition state.

The transition state finally obtained by the LST/QST/conjugate gradient method may not be the transition state connecting the intended reactant and product for a particular reaction step. Therefore, in order to thoroughly investigate the reaction paths, the intrinsic reaction coordinate (IRC) analysis is performed. In DMol^3, the IRC calculations are included in the Transition State Confirmation tool [20]. This tool starts at the transition state and locates successive minima in the direction of the reactant and product paths. This path is known as the minimum energy path, which should connect the supposed transition state to the presumed reactants and products [25]. It uses the nudged elastic band method to validate a transition state by introducing a fictitious spring force which connects the neighbouring points to ensure continuity of the path and then it projects the force, so that the system converges to the minimum energy path [25].

3. Results

In order to investigate the three-step A–E mechanism for methanol oxidation by MDH, models for describing the entire MDH enzyme are selected. Two different models representing the *Methylobacterium extorquens* MDH (1H4I) active site are considered and tested upon methanol oxidation in gas phase. Model A consists of the PQQ molecule, the Ca^{2+} ion and aspartic acid (ASP-303), and model B contains also glutamic acid (GLU-177) and asparagine (ASN-261) in addition to the contents of model A (Figure 3). Then, these active site models are fully optimised and tested upon methanol oxidation following the steps one to three of the A–E mechanism (Figure 2). Reactant (reactant of step 1), Transition states TS1, TS2 and TS3 for steps 1, 2 and 3 respectively, intermediates INT1 (product of step 1) and INT2 (product of step 2), and the final product (product of step 3) optimised structures

are obtained and associated results are presented and discussed in the next section.

4. Structure and bond lengths

4.1 Model A

In model A, the system representing MDH is formed by PQQ, Ca^{2+} and ASP-303. For step one, a methanol molecule is added to that system according to Figure 2 to represent the reactant, and the complete complex is geometry optimised at the BLYP/DNP theory level. Then, the product of step one (INT1) is built according to Figure 2 and geometry optimised at the same level of theory. Finally, transition state search and transition state confirmation calculations are performed as explained in the Methodology section until the transition state (TS1) corresponding to step 1 of the A–E mechanism is found. This procedure is repeated for all three steps in the A–E mechanism. Geometry optimised structures are presented in Figure 4 and selected bond lengths are tabulated in Table 1.

In step 1, the proton (H16) abstraction to O14 of ASP-303 is observed at this theory level, The O14—H16 bond length evolves from 2.18 (reactant) to 1.09 (TS1) to 1.00 (INT1) Å (Table 1), showing the binding of the H16 proton to ASP-303. The C5—O16 distance from the initial reactant is reduced from 4.35 to 2.96 and finally to 1.46 Å, evidencing the formation of the hemiketal intermediate of the rest of methanol with C5 of PQQ. The transition state (TS1) is found to be 22 kcal/mol less stable than the initial reactant complex. The corresponding imaginary frequency ($\sim 95\,cm^{-1}$) corresponds to the translational motion of the CH_3O^- towards the C5 of PQQ and the proton (H16) transferred to the ASP.

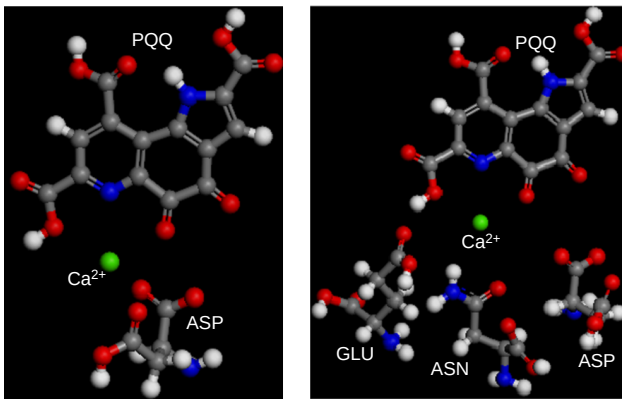

Figure 3. Geometry optimised models representing the *M. extorquens* MDH (1H4I) active site. (a) Model A: PQQ molecule, the Ca^{2+} ion and aspartic acid (ASP-303). (b) Model B: PQQ molecule, the Ca^{2+} ion, aspartic acid (ASP-303), glutamic acid (GLU-177) and asparagine (ASN-261).

In step 2, the second intermediate (INT2) is formed by the H16 proton transfer from ASP-303 to the O5 of PQQ. The CH_3O^- tilts its orientation with respect to INT1 in such a way that the distance between O4 of PQQ and H17 of methanol is 2.51 Å compared to 2.83 Å in INT1. The transition state for this step (TS2) shows an intermediate location of H16 on its way from O14 of ASP to the PQQ carbonyl oxygen O5, with H16—O5 = 1.23 Å and H16—O14 = 1.24 Å (Table 1). This transition state imaginary frequency ($\sim 700\,cm^{-1}$) corresponds to the symmetrical stretching of the O5—H16 and H16—O14 bonds. TS2 is 7 kcal/mol less stable than INT1.

In step 3, the formation of the reduced $PQQH_2$ complex and the final formaldehyde by-product is observed at the BLYP/DNP theory level. The cleavage of the carbon atom in the methanol molecule and H17

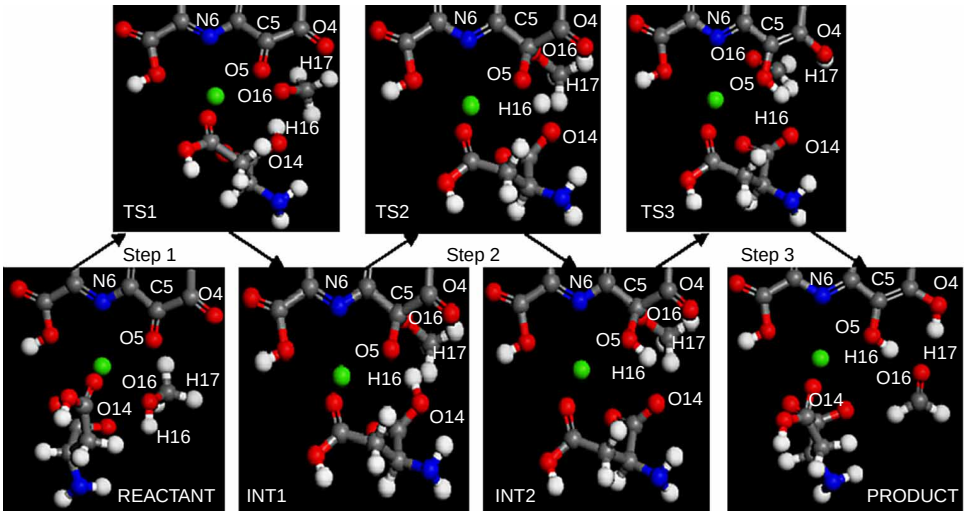

Figure 4. Geometry Optimised structures involved in A–E methanol oxidation mechanism for model A representing the MDH active site.

Table 1. Selected bond lengths corresponding to the optimised structures of reactant (reactant of step one), transition states TS1, TS2 and TS3 for steps one, two and three respectively, intermediates INT1 (product of step 1) and INT2 (product of step 2), and the final product (product of step 3) for models A and B (in parenthesis).

Bond length (Å)	Reactant	TS1	INT1	TS2	INT2	TS3	Product
O14—H16	2.18	1.09	1.00	1.24	1.76	1.73	2.09
	(1.69)	(1.01)	(0.98)	(2.58)	(2.60)	(2.89)	(2.60)
C5—O16	4.35	2.96	1.46	1.48	1.48	3.00	3.52
	(4.10)	(2.75)	(1.40)	(1.48)	(1.49)	(3.39)	(5.33)
O5—H16	3.97	2.66	1.44	1.23	1.01	1.02	1.00
	(3.55)	(3.53)	(3.43)	(2.21)	(1.03)	(1.00)	(1.00)
O4—H17	5.74	3.16	2.83	2.72	2.51	1.21	0.98
	(5.21)	(4.91)	(2.96)	(2.86)	(2.59)	(1.01)	(0.99)
C_{met}—H17	1.10	1.11	1.10	1.10	1.10	1.59	2.58
	(1.10)	(1.11)	(1.10)	(1.10)	(1.10)	(1.47)	(2.82)

is observed since the C_{met}—H17 bond length evolves from 1.10 (INT2) to 1.59 (TS3) to 2.58 (product) and the corresponding H17—O4 distances from 2.51 to 1.21 and to 0.98 Å, respectively. Even though the O4 of PQQ and H17 of methanol appear close to each other (Figure 4) during the previous steps, in reality they are not (Table 1) until this step takes place. Moreover, the distance between O16 of methanol and C5 of PQQ changes from 1.48 to 3.00 and to 3.52 Å, indicating that the formation of the by-product formaldehyde is indeed possible. The transition state for this step (TS3) is 13 kcal/mol less stable than INT2. Its corresponding imaginary frequency ($\sim 430\,cm^{-1}$) corresponds to the movement of the H17 between the methyl carbon (C_{met}) and O4 of PQQ.

4.2 *Model B*

In model B, the system representing MDH is formed by PQQ, Ca^{2+}, ASP-303, GLU-177 and ASN-261. As explained in Section 4.1 for model A, the same procedure is followed to explore the methanol A–E mechanism for model B. Geometry optimised structures are presented in Figure 5 and selected bond lengths tabulated (in parenthesis) in Table 1.

In step 1, the first proton (H16) transfer from methanol to O14 of ASP-303 is observed as well as the hemiketal formation of the rest of the methanol molecule with the C5 of PQQ. The O14—H16 distance reduces from 1.69 to 1.01 and to 0.98 Å, evidencing the first proton transfer to the ASP-303. The C5—O16 bond length variation from 4.10 to 2.76 and to 1.40 Å indicates that the nucleophilic attachment of the rest of the methanol molecule to C5 of PQQ is possible. The transition state for this step is 28 kcal/mol less stable than the reactant. Its imaginary frequency ($\sim 840\,cm^{-1}$) corresponds to the translational motion of the CH_3O^- between the C5 of PQQ and the proton (H16) transferred to the ASP.

In step 2, the H16 proton transfer from O14 of ASP-303 to the PQQ carbonyl oxygen O5 is observed to happen. The O14—H16 bond distance increases from 0.98 to 2.58 and to 2.60 Å, and O5—H16 is decreasing from 3.43 to 2.21 and to 1.03 Å, evidencing that particular proton transfer. The transition state for this step is 5 kcal/mol less stable than the INT1. Its imaginary frequency ($\sim 670\,cm^{-1}$) corresponds to the lateral movement of proton H16 between O14 of ASP-303 and O5 of PQQ.

In step 3, the formation of the reduced $PQQH_2$ complex and the by-product formaldehyde is observed. The bond distance between C5 of PQQ and O16 of methanol increases (Table 1), indicating that the

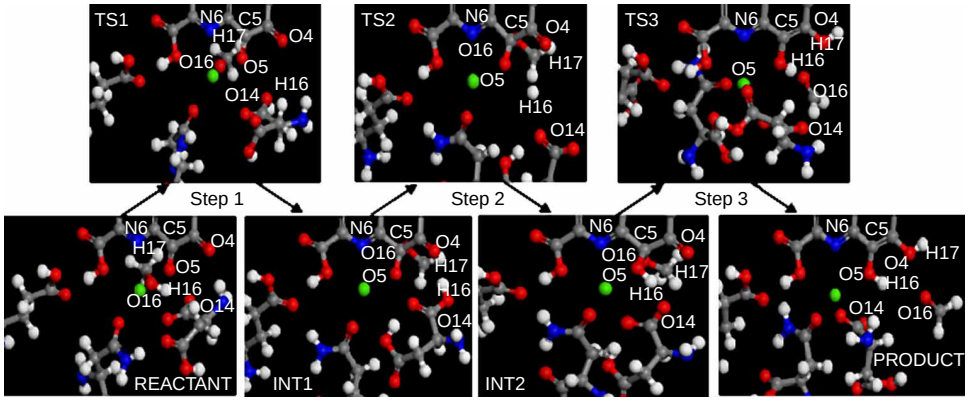

Figure 5. Same as Figure 4 for model B.

formation of formaldehyde is possible. The transition state for this step is 17 kcal/mol less stable than INT2. Its imaginary frequency ($\sim$690 cm^{-1}) corresponds to the movement of the H17 between the methyl carbon (C_{met}) and O4 of PQQ.

5. Effect of model size on structure and energetics

In order to investigate the effect of the model size on the structure of the reactant, transition states, intermediates and product, the bond length difference, $\Delta = d$(model B) $-$ d(model A), is computed for three key distances d = O14—H16, O5—H16 and C_{met}—H17 and plotted for the structures along the reaction path (Figure 6).

The O14—H16 bond length is longer (by 0.50 Å) in case of model A than model B for the reactant. This distance in TS1 and INT1 is practically the same irrespective of the model under consideration, but as the reaction proceeds, this bond length increases by 0.50–1.30 Å in model B with respect to that in model A. The O5—H16 bond length is 0.50 Å longer in model A than that in model B for the reactant. Then, it increases by 0.76–2.00 Å for the complexes of model B relative to the corresponding ones in model A. Finally, this distance is practically the same irrespective of the model under consideration for all complexes of step 3. The C_{met}—H17 bond length is almost the same for all species for the two models considered, except for a slight increase ($\sim$0.25 Å) in the case of the product of step 3. The large bond length differences Δ in the case of O5—H16 and O14—H16 for the two models indicates that this first proton transfer (H16) from methanol to ASP-303 and from ASP-303 to PQQ is indeed affected by the model size, and that unrealistic behaviour might be observed in this case when the size of the MDH active site model is not carefully selected. On the other hand, the second proton (H17) transfer corresponding to the cleavage of C_{met}—H17 is practically unaffected by the MDH active site model under consideration.

Calculated forward and reverse energy barriers for steps 1 to 3 for methanol oxidation by MDH according to the A–E mechanism are tabulated in Table 2. The complete reaction path for both models is shown in Figure 7, where energy values are presented relative to the reactant energy. At the BLYP/DNP theory level, it is evident that step 1 is the slowest (Table 2) with energy barriers of 22 and 28 kcal/mol for models A and B respectively. Step 2 of this mechanism is the fastest, with small energy barriers of 7 and 5 kcal/mol for models A and B, respectively. The energy barriers for the cleavage of the C atom of methanol (C_{met}) and H17 are 13 and 17 kcal/mol for models A and B respectively, in good agreement with the general kinetic requirements of an enzymatic process (15–20 kcal/mol) [17], particularly for the largest model (B).

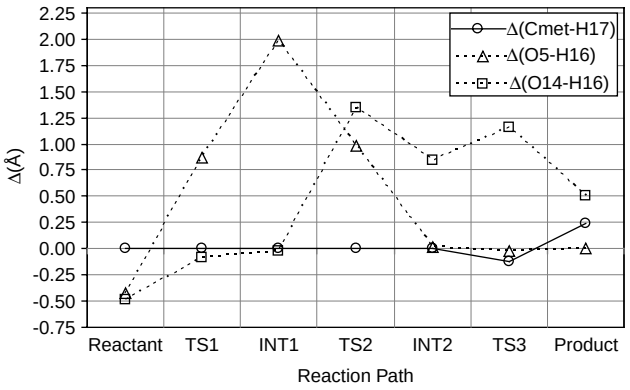

Figure 6. Calculated bond length difference $\Delta = d$(model B) $-$ d(model A) for three key distances d = O14—H16, O5—H16 and C_{met}—H17 along the reaction path.

6. Discussion

The proposed A–E mechanism tested upon the two selected active site models A and B at the BLYP/DNP theory level shows that irrespective of the MDH model under consideration, the conversion of the reactant into the first intermediate (INT1) through TS1 (step 1) is kinetically slower than the final conversion of second intermediates (INT2) to products through TS3 (step 3), and than step 2. However, since step 1 is not kinetically favourable in the gas phase at this theory level, it is possible that either solvent effects are critical or that one or more intermediate steps leading to the formation of the first intermediate complex are missing from the proposed methanol A–E mechanism by MDH. Steps 2 and 3 are kinetically favourable, and between the two, step 3 is the rate-determining step at the BLYP/DNP theory level, which corresponds to the cleavage of the C_{met} and H17 bond in good agreement with experimental observations. The calculated energy barriers (forward) for this step are

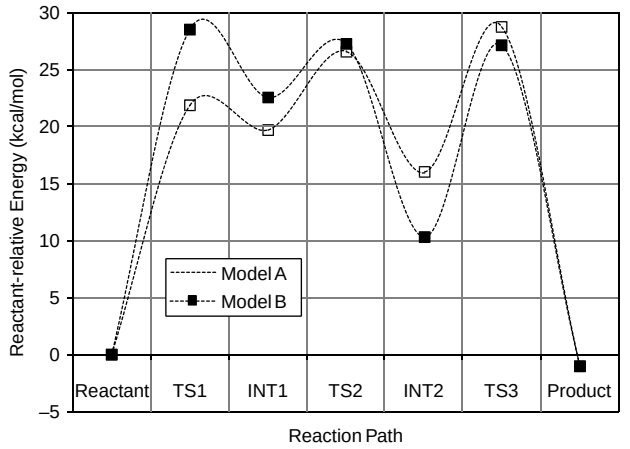

Figure 7. Gas-Phase Potential Energy Surface (PES) for active site models A and B. Reactant-relative energies calculated at the BLPY/DNP theory level are in kcal/mol.

Table 2. Forward and Reverse energy barriers (kcal/mol) corresponding to steps one to three of the A–E methanol oxidation mechanism calculated at the BLPY/DNP theory level for models A and B.

	Model A		Model B	
Step	Forward	Reverse	Forward	Reverse
1	22	2	28	6
2	7	11	5	17
3	13	29	17	28

13 and 17 kcal/mol for models A and B, respectively, which are within the commonly accepted range for enzymatic reactions (15–20 kcal/mol) taking into account the typical error (4–10 kcal/mol) at this level. Moreover, an extra error is anticipated since the calculations presented in this paper were performed in gas phase. The presence of an activator (ammonia) in solvent and/or protein environment could further stabilise the intermediates and transition states, thereby modifying the energy barriers for a possible smoother catalytic process.

7. Conclusions

The A–E reaction mechanism proposed for the methanol oxidation by PQQ-containing MDH was investigated by employing two models representing the active site of the enzyme. The results obtained from the gas-phase calculations demonstrate that the oxidation of methanol can proceed through the A–E mechanism, however step 1 as proposed in the literature is not kinetically favourable at the BLYP/DNP theory level. The rate-determining step (step 3, cleavage of C_{met}—H17) for MDH models A and B shows energy barriers of 13 and 17 kcal/mol respectively in fair agreement with experimental observations. DMol^3 can be used to explore the reaction pathway of the A–E methanol oxidation mechanism by MDH. The BLYP/DNP combination selected for this study is an adequate theory level for obtaining structural information, and a fairly good starting level to be followed by more accurate methods for quantifying the energy barriers for this mechanism.

Acknowledgements

It is gratefully acknowledged the financial support from the National Science Foundation (NSF) under the NSF-CAREER, Grant CTS-0449046. Support for computational resources including software and hardware through the Louisiana Board of Regents, contract LEQSF(2007–08)-ENH-TR-46, the National Science Foundation grant number NSF/IMR DMR-0414903, and the Louisiana Optical Network Initiative (LONI) are also thankfully acknowledged.

References

[1] C. Anthony, *Methanol Dehydrogenase, A PQQ-Containing Quinoprotein Dehydrogenase*, Kluwer Academic/Plenum Publishers, New York, 2000.
[2] M. Ghosh, C. Anthony, K. Harlas, M.G. Goodwin, and C.C.F. Blake, *The refined structure of the quinoprotein methanol dehydrogenase from* Methylobacterium extorquens *at 1.94 Å*, Structure (London) 3 (1995), pp. 1771–1787.
[3] P.R. Afolabi, K. Amaratunga, O. Majekodunmi, S.L. Dales, R. Gill, D. Thompson, J.B. Cooper, S.P. Wood, P.M. Goodwin, and C. Anthony, *Site-directed mutagenesis and X-ray crystallography of the PQQ-containing quinoprotein methanol dehydrogenase and its electron acceptor, cytochrome CL*, Biochem. J. 40 (2001), pp. 9799–9809.
[4] S. White, G. Boyd, F.S. Mathews, Z.X. Xia, W.W. Dai, Y.S. Zhang, and V.L. Davidson, *The active site structure of calcium containing methanol dehydrogenase*, J.Biochem. 32 (1993), pp. 12955–12958.
[5] Z.X. Xia, W.W. Dai, J.P. Xiong, Z.P. Hao, V.L. Davidson, S. White, and F.S. Mathews, *The three-dimensional structures of methanol dehydrogenase from two methylotrophic bacteria at 2.6 Å resolution*, J. Biol. Chem. 267 (1992), pp. 22289–22297.
[6] Z.X. Xia, Y.N. He, W.W. Dai, S. White, G. Boyd, and F.S. Mathews, *Detailed active site configuration of a new crystal form of methanol dehydrogenase from* Methylophilus W3a1 *at 1.9 Å resolution*, Biochem. J. 38 (1999), pp. 1214–1220.
[7] C. Anthony and P. Williams, *The structure and mechanism of methanol dehydrogenase*, Biochim. Biophys. Acta 1647 (2003), pp. 18–23.
[8] A. Oubrie, H.J. Rozeboom, K.H. Kalk, A.J. Olsthoorn, J.A. Duine, and B.W. Dijkstra, *Structure and mechanism of soluble quinoprotein glucose dehydrogenase*, EMBO J. 18 (1999), pp. 5187–5194.
[9] A.R. Dewanti and J.A. Duine, *Ca^{2+}-assisted, direct hydride transfer, and rate-determining tautomerization of C5-reduced PQQ to PQQH2, in the oxidation of beta-D-glucose by soluble, quinoprotein glucose dehydrogenase*, Biochem. J. 39 (2000), pp. 9384–9392.
[10] A. Oubrie, H.J. Rozeboom, K.H. Kalk, E.J. Huizinga, and B.W. Dijkstra, *Crystal structure of quinohemoprotein alcohol dehydrogenase from Comamonas testosteroni; structural basis for substrate oxidation and electron transfer*, J. Biol. Chem. 277 (2002), pp. 3727–3732.
[11] J. Frank, S.H. van Krimpen, P.E. J. Verwiel, J.A. Jongejan, and A.C. Mulder, *On the mechanism of inhibition of methanol dehydrogenase by cyclopropane-derived inhibitors*, Eur. J. Biochem. 184 (1989), pp. 187–195.
[12] A.J. J. Olsthoorn and J.A. Duine, *On the mechanism and specificity of the soluble, quinoprotein glucose dehydrogenase in the oxidation of aldose sugars*, Biochemistry 37 (1998), pp. 13854–13861.
[13] J. Frank, M. Dijkstra, J.A. Duine, and C. Balny, *Kinetic and spectral studies on the redox forms of methanol dehydrogenase from Hyphomicrobium X*, Eur. J. Biochem. 174 (1988), pp. 331–338.
[14] S. Itoh, H. Kawakami, and S. Fukuzumi, *Model studies on calcium-containing quinoprotein alcohol dehydrogenases. Catalytic role of Ca^{2+} for the oxidation of alcohols by coenzyme PQQ (4,5 dihydro-4,5-dioxo-1h-pyroolo[2,3-F]quinoline-2,7,9-tricarboxylic acid)*, J. Biochem. 37 (1998).
[15] S. Itoh, H. Kawakami, and S. Fukuzumi, *Development of the active site model for calcium-containing quinoprotein alcohol dehydrogenases*, J. Mol. Catal. B 8 (2000), pp. 85–94.
[16] M.G. Goodwin and C. Anthony, *Characterization of a novel methanol dehydrogenase containing a Ba^{2+} ion at the active site*, Biochem. J. 318 (1996), pp. 673–679.
[17] M. Leopoldini, N. Russo, and M. Toscano, *The preferred reaction path for the oxidation of methanol by pqq-containing methanol dehydrogenase: Addition–elimination versus hydride-transfer mechanism*, Chem. Eur. J. 13 (2007), pp. 2109–2117.
[18] J.P. Perdew, *Electronic Structure of Solids*, Akademie Verlag, Berlin, 1991.
[19] R.M. Dreialer and E.K.U. Gross, *Density Functional Theory: An Approach to Quantum Many Body Problem*, Springer, Berlin, 1990.
[20] Accelrys, Inc Materials Studio (2006).

[21] C. Lee, W. Yang and R. Parr, *Development of the Colle-Salvetti correlation-energy formula into a functional of the electron density*, Phys. Rev. B 37 (1998), pp. 786–789.
[22] Accelrys, Inc DMol3 User Guide (2003).
[23] W. Koch and M.C. Holthausen, *A Chemist's Guide to Density Functional Theory*, Wiley-VCH, Weinheim, 2001.
[24] N. Govind, M. Petersen, G. Fitzgerald, D. King-Smith, and J. Andzelm, *A generalized synchronous transit method for transition state location*, Comput. Mater. Sci. 28 (2003), pp. 250–258.
[25] M. Grillo, N. Govind, G. Fitzgerald, and K.B. Stark, *Computational material science with materials studio: Applications in catalysis*, Lect. Notes Phys. 642 (2004), pp. 202–227.